Quantum Fluctuation Dynamics of Dispersive Superradiant Pulses in a Hybrid Light-Matter System

Kevin C. Stitely,[1,2,3,*] Fabian Finger,[4] Rodrigo Rosa-Medina,[4] Francesco Ferri,[4] Tobias Donner,[4] Tilman Esslinger,[4] Scott Parkins,[1,3] and Bernd Krauskopf[1,2]

[1]*Dodd-Walls Centre for Photonic and Quantum Technologies, New Zealand*
[2]*Department of Mathematics, University of Auckland, Auckland 1010, New Zealand*
[3]*Department of Physics, University of Auckland, Auckland 1010, New Zealand*
[4]*Institute for Quantum Electronics and Quantum Center, ETH Zürich, 8093 Zürich, Switzerland*

(Received 19 February 2023; accepted 6 September 2023; published 6 October 2023)

We consider theoretically a driven-dissipative quantum many-body system consisting of an atomic ensemble in a single-mode optical cavity as described by the open Tavis-Cummings model. In this hybrid light-matter system, the interplay between coherent and dissipative processes leads to superradiant pulses with a buildup of strong correlations, even for systems comprising hundreds to thousands of particles. A central feature of the mean-field dynamics is a self-reversal of two spin degrees of freedom due to an underlying time-reversal symmetry, which is broken by quantum fluctuations. We demonstrate a quench protocol that can maintain highly non-Gaussian states over long timescales. This general mechanism offers interesting possibilities for the generation and control of complex fluctuation patterns, as suggested for the improvement of quantum sensing protocols for dissipative spin amplification.

DOI: 10.1103/PhysRevLett.131.143604

In recent years, there has been considerable interest in driven-dissipative quantum many-body systems, which appear in fields ranging from atomic and optical physics [1] to condensed matter [2] and quantum information theory [3]. The in- and outflux of energy, essential for applications, significantly modifies the dynamics that quantum systems admit. Examples exploiting the interplay between coherence and dissipation range from limit-cycle and time-crystalline behavior [4–8], superradiant oscillations [9,10], and chaos [11–13] to dissipation-induced and topological phases [14–17]. Studies of many-body nonequilibrium quantum systems typically focus on mean-field behavior where quantum fluctuations are small. Moreover, treatments of fluctuations are usually concerned with steady-state effects, such as critical exponents in the vicinity of quantum phase transitions [18–20]. Studies of the *dynamics of quantum fluctuations* in driven-dissipative quantum systems have so far been limited to spin squeezing [21–24]. Recently, there has been much interest in the dissipation-engineered creation and control of fluctuations, suggesting that, rather than being detrimental to entanglement, dissipation can, in fact, be harnessed for applications [25–27].

In this work, we explore the fluctuation dynamics of an atomic ensemble coupled to a single-mode optical cavity via a driving laser field [Figs. 1(a) and 1(b)]. This system, described by the dissipative Tavis-Cummings model [28], has been thoroughly investigated in its limiting cases where dissipation is either dominant, leading to superradiant decay [29], or practically nonexistent, inducing spin-squeezing dynamics [22,30]. We show that, in the unexplored regime between these two extremes, the interplay of coherent and dissipative interactions leads to non-Gaussian fluctuations, during what we term *dispersive superradiant pulses* [Fig. 1(c)]. Here, higher-order quantum fluctuations remain significant even as the system size

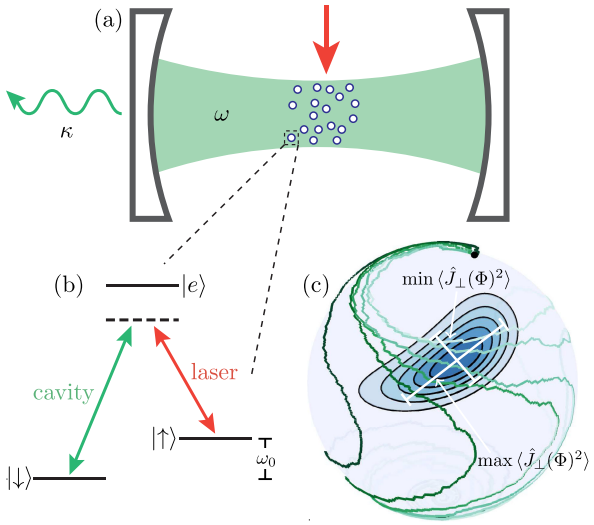

FIG. 1. (a) Schematic of the open Tavis-Cummings model. (b) Atomic energy level and coupling configuration. (c) Dispersive superradiant pulse illustrated on the atomic Bloch sphere by six quantum trajectories and the spin Q function; here, $\kappa = 1$, $\lambda = 0.5$, and $N = 200$, with initial state $|\theta_0, \phi_0\rangle = |\pi/10, \pi/2\rangle$.

increases toward a regime where one might naïvely expect the thermodynamic limit to take hold. Moreover, this dissipative system possesses an unusual symmetry on the mean-field level, resulting from the combined inversion of time and population difference, which is broken by quantum fluctuations. Finally, we demonstrate that quenching the effective cavity resonance and light-matter coupling can preserve highly non-Gaussian states over surprisingly long timescales.

We consider N atoms inside a single-mode optical cavity with effective resonance frequency ω and decay rate κ. The atoms are in a Λ configuration with two (nominal) ground states $|\downarrow\rangle$ and $|\uparrow\rangle$ and an excited state $|e\rangle$ [Figs. 1(a) and 1(b)] and are driven with a cavity-assisted Raman transition: A laser couples to the transition $|\uparrow\rangle \leftrightarrow |e\rangle$, while $|\downarrow\rangle \leftrightarrow |e\rangle$ is coupled to the cavity mode. The atoms are fixed in place at alternate antinodes of the field and couple identically. If the driving laser and cavity mode are far detuned from atomic resonance, $|e\rangle$ can be adiabatically eliminated. The coupling scheme can then be seen as a two-photon transition between $|\downarrow\rangle$ and $|\uparrow\rangle$, facilitated by a laser and a cavity photon. The system is captured by the Tavis-Cummings Hamiltonian [28] (with $\hbar = 1$)

$$\hat{H}_{\mathrm{TC}} = \omega \hat{a}^\dagger \hat{a} + \omega_0 \hat{J}_z + \frac{\lambda}{\sqrt{N}}(\hat{a}\hat{J}_+ + \hat{a}^\dagger \hat{J}_-), \qquad (1)$$

where $\hat{a}$ is the annihilation operator of the cavity field mode with effective frequency ω, $\hat{J}_{\pm,z}$ are collective spin-$N/2$ operators, ω_0 is the effective energy level splitting, and λ is the light-matter coupling strength. The primary dissipative mechanism of this open quantum system is leakage of cavity photons, which we model with the Lindblad master equation

$$\frac{d\hat{\rho}}{dt} = -i[\hat{H}_{\mathrm{TC}}, \hat{\rho}] + \kappa(2\hat{a}\,\hat{\rho}\,\hat{a}^\dagger - \hat{a}^\dagger \hat{a}\,\hat{\rho} - \hat{\rho}\hat{a}^\dagger \hat{a}), \qquad (2)$$

where $\hat{\rho}$ is the reduced density operator and κ is the cavity decay rate. By adiabatically eliminating the cavity field mode (assuming $\sqrt{\omega^2 + \kappa^2} \gg \lambda, \omega_0$) [30,31] and taking a rotating frame [32], we arrive at a one-axis twisting Hamiltonian:

$$\hat{H} = -\frac{\xi \lambda^2}{N}\left(\frac{N^2}{4} - \hat{J}_z^2\right), \qquad (3)$$

with the master equation

$$\frac{d\hat{\rho}}{dt} = -i[\hat{H}, \hat{\rho}] + \frac{\eta \lambda^2}{N}(2\hat{J}_-\hat{\rho}\hat{J}_+ - \hat{J}_+\hat{J}_-\hat{\rho} - \hat{\rho}\hat{J}_+\hat{J}_-). \qquad (4)$$

Here, $\xi = \omega/(\kappa^2 + \omega^2)$, $\eta = \kappa/(\kappa^2 + \omega^2)$, and $\hat{\rho}$ is now the reduced density operator of the atom-only system. Equation (3) describes the effective global-range spin-spin interactions within the ensemble, mediated by cavity photons. In Eq. (4), cavity dissipation gives rise to a collectively enhanced population inversion toward the spin state $\bigotimes_{j=1}^{N} |\downarrow_j\rangle$, i.e., Dicke superradiance [29,34]. Since Eqs. (3) and (4) conserve the collective spin length, the dynamics can be represented as the evolution of a quasiprobability distribution on the surface of the Bloch sphere [Fig. 1(c)], which we capture by the Husimi spin Q function [32]. In the semiclassical limit $N \to \infty$, fluctuations become negligible (the quasiprobability distribution tends to a δ distribution) and the dynamics are described by the mean-field trajectories $\langle \hat{J}_x(t)\rangle$, $\langle \hat{J}_y(t)\rangle$, and $\langle \hat{J}_z(t)\rangle$, confined onto the Bloch sphere [32].

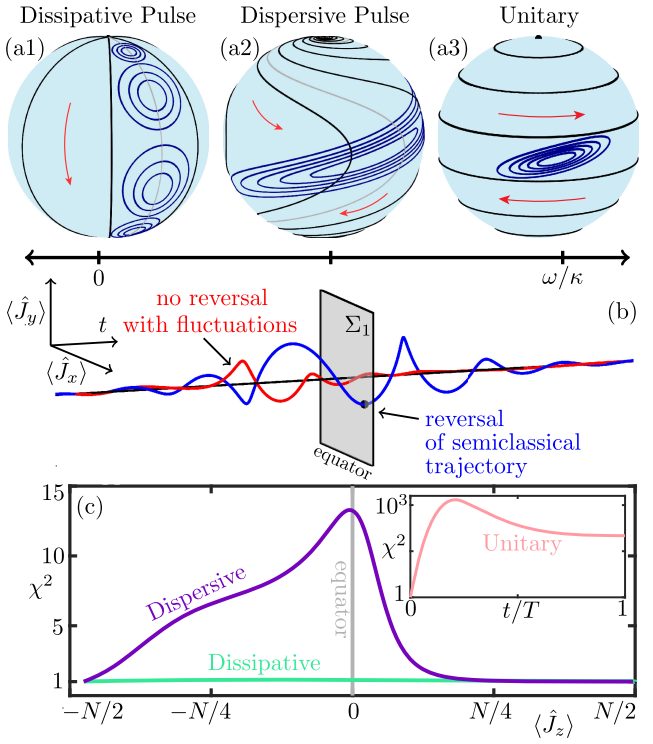

FIG. 2. (a) Semiclassical trajectories (black) and contours of the spin Q function (blue) during the system's evolution on the Bloch sphere for dissipative (a1) and dispersive (a2) pulses initialized at $|\theta_0, \phi_0\rangle = |\pi/10, \pi/2\rangle$ and for the unitary case (a3) at $|\pi/2, \pi/2\rangle$. (b) Inversion-time-reversal symmetry (blue line) is broken by quantum fluctuations (red line). (c) Deformation parameter χ^2 as a function of the inversion $\langle \hat{J}_z(t)\rangle$ for $\omega = 0$ (dissipative) and for $\omega = 5$ (dispersive); inset: χ^2 versus time for the unitary case with $\omega = 5$, $\kappa = 0$, and integration time $T = 800$. For all, $\lambda = 0.5$ and $N = 200$.

The open Tavis-Cummings model has been studied when the dynamics are either purely dissipative [34–39] or purely coherent (unitary) [22,40–43]. The former case ($\omega/\kappa = 0$) reduces to the superradiance master equation [34,38]. Here, semiclassical trajectories move to the south pole along longitudinal lines [Fig. 2(a1)]. Fluctuations increase uniformly in all spin directions due to the curvature of the Bloch sphere. The purely coherent case ($\omega/\kappa \to \infty$), on

the contrary, has no dissipative term and exhibits spin-squeezing dynamics [21,22,30]. The semiclassical trajectories form latitudinal circles corresponding to Rabi oscillations [Fig. 2(a3)], without emission into the cavity, and have an inversion-dependent Rabi frequency of $2\xi\lambda^2\langle\hat{J}_z\rangle/N$; see Eq. (3)—leading to spin squeezing at the equator [Fig. 2(a3)].

In the intermediate range $0 < \omega/\kappa < \infty$, the interplay between superradiant-pulsed behavior via dissipation and Rabi oscillations from a cavity-atom detuning gives rise to rich dynamics of dispersive superradiant pulses. Here, semiclassical trajectories unwind down the Bloch sphere and reverse direction at the equator [Fig. 2(a2)], approaching the south pole. When the mean spin direction is at the equator, the (instantaneous) Rabi frequency is zero and becomes negative. This results in partial self-reversal of the trajectories, which stems from the *inversion-time-reversal symmetry* $\mathcal{T}_1$: $(t, \langle\hat{J}_z\rangle) \mapsto (-t, -\langle\hat{J}_z\rangle)$ [32]. Hence, any trajectory that intersects the symmetry subspace $\Sigma_1 = \{(\langle\hat{J}_x\rangle, \langle\hat{J}_y\rangle, \langle\hat{J}_z\rangle) \in \mathbb{S}^2 | \langle\hat{J}_z\rangle = 0\}$ is invariant under $\mathcal{T}_1$ [44,45]. In other words, $\langle\hat{J}_x\rangle$ and $\langle\hat{J}_y\rangle$ undergo a reversal of their dynamics when the equator is crossed.

Since every trajectory tends toward the south pole of the Bloch sphere, any initially excited trajectory $[\langle\hat{J}_z(0)\rangle > 0]$ is guaranteed to intersect Σ_1 and will, thus, be symmetric under inversion-time reversal. Unlike existing protocols for engineering time-reversal dynamics, which require external modification (flipping the sign of the Hamiltonian) [46–48], this system is intrinsically *self-reversing* in the spin components $\langle\hat{J}_x\rangle$ and $\langle\hat{J}_y\rangle$ [Fig. 2(b)]. Surprisingly, this is dissipation induced: Since the Rabi frequency at the equator is zero, motion through Σ_1 is purely dissipative. Note that simultaneous self-reversal of all spin components is impossible, as it would violate the uniqueness theorem for ordinary differential equations [49,50]. Rather, only $\langle\hat{J}_x\rangle$ and $\langle\hat{J}_y\rangle$ self-reverse, while $\langle\hat{J}_z\rangle$ evolves monotonically to $\langle\hat{J}_z\rangle = -N/2$.

Simulation of Eq. (4) reveals that quantum fluctuations break inversion-time-reversal symmetry [Fig. 2(b)], connected with the appearance of highly non-Gaussian spin states during dispersive superradiant pulses [Figs. 1(c) and 2(a2)] with a large enhancement of fluctuations in one quadrature. The physical origin of the nonuniform state expansion can be understood by taking a quantum trajectories approach [51,52]. Figure 1(c) shows six quantum trajectories initialized in a spin coherent state $|\theta_0, \phi_0\rangle = |\pi/10, \pi/2\rangle$. The positive divergence of the semiclassical equations in the northern portion of the Bloch sphere results in the amplification of the fluctuations of quantum trajectories during the initial stage of the pulse [32]. This "fanning out" of trajectories causes the enhancement of fluctuations in certain directions. Once the mean spin direction crosses the equator, the trajectories converge, so the overall level of fluctuations is reduced.

To describe the nonuniform expansion, we introduce the *deformation parameter*

$$\chi^2 = \frac{\max_\Phi \langle \Delta\hat{J}_\perp(\Phi)^2\rangle}{\min_\Phi \langle \Delta\hat{J}_\perp(\Phi)^2\rangle} \geq 1, \tag{5}$$

where $\langle \Delta\hat{J}_\perp(\Phi)^2\rangle$ is the spin variance in a direction orthogonal to the mean spin direction, parametrized by the angle Φ, relative to the longitudinal direction. Figure 2(c) shows χ^2 during a purely dissipative and a dispersive pulse. In the dissipative case, the state expands uniformly [Fig. 2(a1)] and $\chi^2 \approx 1$ throughout. Without dissipation, states initiated at the equator are eventually oversqueezed into non-Gaussian states, leading to very large χ^2 [Fig. 2(c), inset]. The dispersive case has a clear initial rise in χ^2, then peaks, and quickly decreases as the system approaches its steady state ($\langle\hat{J}_z\rangle \to -N/2$) with uniform fluctuations. The (nonequilibrium) steady state is the spin coherent state at the south pole $|\theta, \phi\rangle = |\pi, \phi\rangle$ which is also a dark state of the jump operator $\hat{J}_-$, i.e., $\hat{J}_-|\pi, \phi\rangle = 0$. Figure 2(c) also demonstrates that quantum fluctuations break inversion-time symmetry, since χ^2 is not symmetric about $\langle\hat{J}_z\rangle = 0$.

We apply a cumulant expansion approach to further investigate these emerging non-Gaussian quantum states, as shown in Figs. 1(c) and 2(a2). Also known as connected correlation functions [53] or Ursell functions [54], cumulants quantify the effects of higher-order moments by subtracting out redundant information determined by moments of lower order. They have been used recently as the basis for a truncation method in a variety of contexts [55–61], in particular, to study superradiance and squeezing in many-body quantum systems [62–64].

In typical light-matter interaction models, the equations of motion for moments at the order of n depend on the moments at the order of $n+1$, thus creating an infinite hierarchy of differential equations. In the nth cumulant expansion, one assumes that the cumulants at the order of $n+1$ vanish, thus closing the system of equations. The first-order expansion describes the semiclassical (mean-field) approximation, which is valid when the strength of fluctuations is small. The second-order cumulant expansion, with cumulants $\langle\hat{J}_j\hat{J}_k\rangle_c = \langle\hat{J}_j\hat{J}_k\rangle - \langle\hat{J}_j\rangle\langle\hat{J}_k\rangle$, $j, k \in \{x, y, z\}$, is valid for approximately Gaussian states and enables investigations of fluctuations, e.g., for spin squeezing. The buildup of third-order cumulants

$$\begin{aligned}\langle\hat{J}_j\hat{J}_k\hat{J}_\ell\rangle_c = {} & \langle\hat{J}_j\hat{J}_k\hat{J}_\ell\rangle - \langle\hat{J}_j\rangle\langle\hat{J}_k\hat{J}_\ell\rangle - \langle\hat{J}_k\rangle\langle\hat{J}_j\hat{J}_\ell\rangle \\ & - \langle\hat{J}_\ell\rangle\langle\hat{J}_j\hat{J}_k\rangle + 2\langle\hat{J}_j\rangle\langle\hat{J}_k\rangle\langle\hat{J}_\ell\rangle,\end{aligned} \tag{6}$$

with $j, k, \ell \in \{x, y, z\}$, thus signals the appearance of non-Gaussianity. Since correlations shift between cumulants of

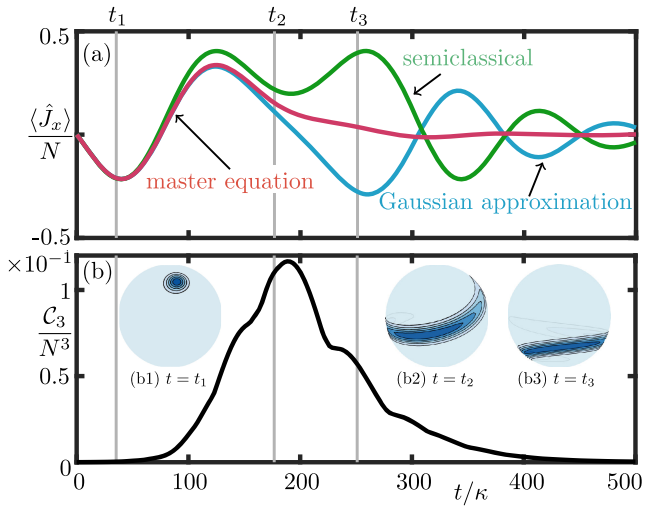

FIG. 3. Generation of non-Gaussian correlations in a dispersive superradiant pulse. (a) Semiclassical (green line), second-order cumulant (blue line), and master equation (red line) computations of $\langle \hat{J}_x(t) \rangle$. (b) Total degree of correlation at third-order $\mathcal{C}_3(t)$. (b1)–(b3) Snapshots of the spin Q function at different times of the pulse, with $|\theta_0, \phi_0\rangle = |\pi/10, \pi/2\rangle$ and $\kappa = 1, \omega = 5, \lambda = 0.5$, and $N = 200$.

different operator permutations dynamically, we define the *total degree of correlation at third order*

$$\mathcal{C}_3(t) = \sum_{j,k,\ell} |\langle \hat{J}_j \hat{J}_k \hat{J}_\ell \rangle_c| \tag{7}$$

by summing over all possible cumulant permutations.

The time evolution of $\langle J_x \rangle$ and $\mathcal{C}_3$ during a dispersive superradiant pulse is shown in Figs. 3(a) and 3(b), using the semiclassical, second-order cumulant expansion, and the full master equation. When the state is approximately coherent [Fig. 3(b1)], $\mathcal{C}_3$ is small and the semiclassical and Gaussian approximations hold. Near the midpoint of the pulse, correlations build up and the state becomes highly non-Gaussian [Fig. 3(b2)], leading to failure of the second-order cumulant expansion (Gaussian approximation) [Fig. 3(a)]. The final state is again a coherent spin state, for which $\mathcal{C}_3 \to 0$. In the second-order cumulant expansion, inversion-time-reversal symmetry is reflected by invariance under the transformation $\mathcal{T}_2 : (t, \langle \hat{J}_z \rangle, \langle \hat{J}_z \hat{J}_\ell \rangle) \mapsto (-t, -\langle \hat{J}_z \rangle, -\langle \hat{J}_z \hat{J}_\ell \rangle)$, where $\ell \in \{x, y\}$. The corresponding symmetry subspace features the additional conditions $\langle \hat{J}_z \hat{J}_\ell \rangle = 0$. Contrary to the semiclassical case, where expectation factorization ensures $\langle \hat{J}_z \hat{J}_\ell \rangle = 0$ if $\langle \hat{J}_z \rangle = 0$, these are generally not satisfied for higher orders. As a result, trajectories will generally not feature inversion-time-reversal symmetry with quantum fluctuations.

So far, we studied the dissipative generation of non-Gaussian states for $N = 200$. However, many cold atom experiments operate in the regime $N > 10^3$ [65].

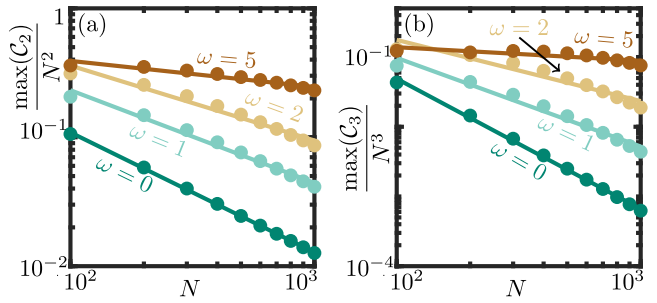

FIG. 4. Scaling of maximum correlations with N at second order (a) and third order (b). The initial state is $|\theta_0, \phi_0\rangle = |\pi/10, \pi/2\rangle$ with $\kappa = 1$ and $\lambda = 0.5$.

Surprisingly, strong correlations created in the dispersive regime decay slowly as the atom number N is increased. Figures 4(a) and 4(b) show how the maximum total degree of normalized correlations at order two, $\max(\mathcal{C}_2)/N^2$, and three, $\max(\mathcal{C}_3)/N^3$, scale with N as ω is varied. Note that we are using the full master equation for computations of $\mathcal{C}_2$ and $\mathcal{C}_3$. Linear fits over a logarithmic scale demonstrate an approximate power law. The purely dissipative case ($\omega = 0$) has the largest gradient (magnitude), with correlations falling off rapidly (approximately $\propto 1/N$), which is compatible with the behavior of coherent states. For larger ω, both second- and third-order correlations $\max(\mathcal{C}_2)/N^2$ and $\max(\mathcal{C}_3)/N^3$ (Fig. 4) are maintained for significantly larger atom numbers, as the pulses become increasingly more dispersive. In this regime, we observe the formation of non-Gaussian states for systems with up to at least $N = 1000$ particles. The onset of classical behavior, in the sense that higher-order cumulants vanish as N increases, occurs for dissipative superradiant pulses well before dispersive pulses. Interestingly, this indicates that, for typical atom numbers in cold atom experiments, a regime exists where even for large $N \gtrsim 10^3$ the full distribution of quantum fluctuations must be taken into account.

In the transient dispersive pulses discussed so far, non-Gaussian states appear and disappear rapidly together with the population inversion. We propose a viable protocol to generate and maintain the shape of non-Gaussian states for long times. Our scheme relies on quenching both the effective cavity resonance ω and coupling λ, as the cavity decay rate κ is fixed experimentally. When the mean spin direction is roughly at the equator of the Bloch sphere, so that non-Gaussian correlations are maximal, ω and λ are ramped down. In this way, a dispersive pulse becomes dissipative and the evolution is slowed, thereby preserving non-Gaussian correlations (Fig. 5). Recent examples of experiments showcasing a precise control of coherent and dissipative couplings are Refs. [4,17,66]. To account for experimentally feasible, noninstantaneous quenches, we model the quenching protocol with a piecewise linear ramp in ω and λ [32]. Initially, the pulse has a dispersive stage with $\omega = \omega_{\max}$ and $\lambda = \lambda_{\max}$. The initially excited atoms

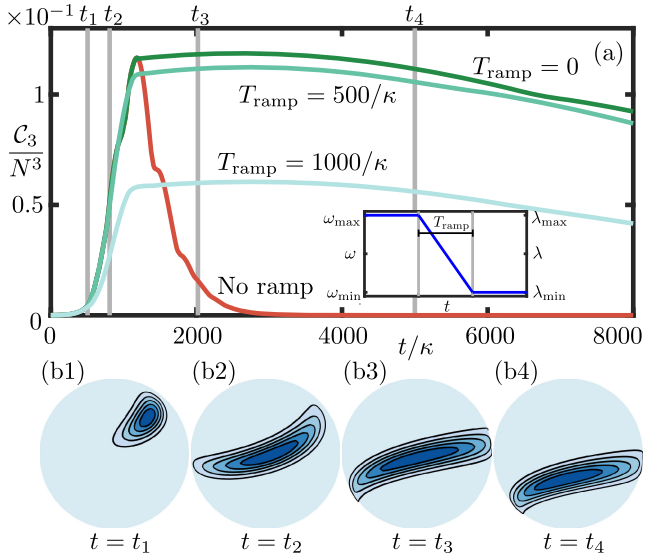

FIG. 5. Preserving non-Gaussian correlations with a quench protocol. (a) $\mathcal{C}_3(t)$ for no ramp (red line), an instantaneous ramp (dark green line), and for ramp times $T_{\mathrm{ramp}} = 500/\kappa$ and $1000/\kappa$ (lighter green lines). The quench protocol is shown in the inset. (b1)–(b4) Snapshots of spin Q function for $T_{\mathrm{ramp}} = 500/\kappa$. Here, $\kappa = 1$, $\omega_{\mathrm{max}} = 5$, $\omega_{\mathrm{min}} = 0$, $\lambda_{\mathrm{max}} = 0.2$, $\lambda_{\mathrm{min}} = 0.02$, $N = 200$, and the initial state is $|\theta_0, \phi_0\rangle = |\pi/10, \pi/2\rangle$.

evolve as in Fig. 3 and begin to exhibit strong correlations, signaling the appearance of non-Gaussianity. When the correlations reach their peak near the midpoint of the pulse, ω and λ are ramped down linearly over a time T_{ramp} to a dissipative stage with $\omega = \omega_{\mathrm{min}}$ and $\lambda = \lambda_{\mathrm{min}}$. In a purely dissipative regime with $\omega_{\mathrm{min}} = 0$, the non-Gaussian state formed over the initial dispersive stage of the pulse is "frozen" and transported down the Bloch sphere as in Fig. 2(a1). Since the speed is determined by λ, a quench can maintain the non-Gaussian states formed in the dispersive stage of the pulse over long periods of time. The preservation of correlations is monitored with $\mathcal{C}_3(t)$ in Fig. 5(a), with the quenching protocol shown in the inset. With no ramping, the superradiant pulse remains dispersive, and there is a rapid buildup of correlations which then disappear quickly. For maintaining non-Gaussian correlations, the best-case scenario is an instantaneous quench with $T_{\mathrm{ramp}} = 0$. In this case, we observe a rapid onset of correlations in the dispersive stage and then, in the dissipative stage, a decay that preserves third-order correlations over a long timescale (ensured by setting $\lambda_{\mathrm{min}}/\lambda_{\mathrm{max}} \ll 1$). For a more realistic quench with finite T_{ramp} (the time taken for the driving laser to change frequency and power), we observe similar behavior, with the maximal degree of correlation only slightly below the instantaneous quench. The evolution of quantum states on the Bloch sphere for $T_{\mathrm{ramp}} = 500/\kappa$ is shown in Figs. 5(b1)–5(b4), showcasing the dispersive stage, followed by a very slow decay of the state.

In conclusion, we have investigated a regime of the open Tavis-Cummings model where a combination of coherent and dissipative processes gives rise to superradiant pulses with highly non-Gaussian quantum correlations. Importantly, enhanced higher-order fluctuations are largely preserved with increasing atom number, showing that the quantum-to-classical crossover can depend strongly on the dynamical behavior of fluctuations. Our results open up exciting possibilities for generation and control of specified non-Gaussian correlations in driven-dissipative many-body quantum systems. The dissipation-robust non-Gaussian quantum states studied could be used in optimal state preparation in quantum metrology [67]. Owing to the strong state deformation, the dispersive regime might be exploited to improve solid-state quantum sensors using superradiant spin amplification [37], to mitigate increases in intrinsic quantum noise via dissipation, or provide benefit to superradiance-based microwave pulse sensors [68]. Its implementation with ultracold atoms in the dispersive regime of cavity QED [9,17] has several advantages. Since cavity detuning and coupling strength are determined by the properties of the drive laser, the parameters we considered can indeed be adjusted dynamically during the experiment. Moreover, it is possible to nondestructively measure the cavity output field, enabling real-time readout of the spin inversion, which is crucial for optimal superradiant spin amplification.

We acknowledge funding from the Swiss National Science Foundation: Projects No. IZBRZ2 186312, No. 182650, No. 212168, and No. 20QT-1_205584 and National Centre of Competence in Research Quantum Science and Technology, from EU Horizon 2020: European Research Council advanced grant TransQ (Project No. 742579).

*kevin.stitely@auckland.ac.nz

[1] T. Langen, R. Geiger, and J. Schmiedmayer, Ultracold atoms out of equilibrium, Annu. Rev. Condens. Matter Phys. **6**, 201 (2015).
[2] I. Carusotto and C. Ciuti, Quantum fluids of light, Rev. Mod. Phys. **85**, 299 (2013).
[3] P. M. Harrington, E. J. Mueller, and K. W. Murch, Engineered dissipation for quantum information science, Nat. Rev. Phys. **4**, 660 (2022).
[4] N. Dogra, M. Landini, K. Kroeger, L. Hruby, T. Donner, and T. Esslinger, Dissipation-induced structural instability and chiral dynamics in a quantum gas, Science **366**, 1496 (2019).
[5] E. I. R. Chiacchio and A. Nunnenkamp, Dissipation-Induced Instabilities of a Spinor Bose-Einstein Condensate Inside an Optical Cavity, Phys. Rev. Lett. **122**, 193605 (2019).
[6] B. Buča, J. Tindall, and D. Jaksch, Non-stationary coherent quantum many-body dynamics through dissipation, Nat. Commun. **10**, 1730 (2019).

[7] H. Keßler, P. Kongkhambut, C. Georges, L. Mathey, J. G. Cosme, and A. Hemmerich, Observation of a Dissipative Time Crystal, Phys. Rev. Lett. **127**, 043602 (2021).
[8] F. Carollo and I. Lesanovsky, Exact solution of a boundary time-crystal phase transition: Time-translation symmetry breaking and non-Markovian dynamics of correlations, Phys. Rev. A **105**, L040202 (2022).
[9] Z. Zhiqiang, C. H. Lee, R. Kumar, K. J. Arnold, S. J. Masson, A. S. Parkins, and M. D. Barrett, Nonequilibrium phase transition in a spin-1 Dicke model, Optica **4**, 424 (2017).
[10] K. C. Stitely, S. J. Masson, A. Giraldo, B. Krauskopf, and S. Parkins, Superradiant switching, quantum hysteresis, and oscillations in a generalized Dicke model, Phys. Rev. A **102**, 063702 (2020).
[11] C. Emary and T. Brandes, Chaos and the quantum phase transition in the Dicke model, Phys. Rev. E **67**, 066203 (2003).
[12] C. Emary and T. Brandes, Quantum Chaos Triggered by Precursors of a Quantum Phase Transition: The Dicke Model, Phys. Rev. Lett. **90**, 044101 (2003).
[13] K. C. Stitely, A. Giraldo, B. Krauskopf, and S. Parkins, Nonlinear semiclassical dynamics of the unbalanced, open Dicke model, Phys. Rev. Res. **2**, 033131 (2020).
[14] M. Soriente, T. Donner, R. Chitra, and O. Zilberberg, Dissipation-Induced Anomalous Multicritical Phenomena, Phys. Rev. Lett. **120**, 183603 (2018).
[15] D. Dreon, A. Baumgärtner, X. Li, S. Hertlein, T. Esslinger, and T. Donner, Self-oscillating pump in a topological dissipative atom–cavity system, Nature (London) **608**, 494 (2022).
[16] S. Diehl, E. Rico, M. A. Baranov, and P. Zoller, Topology by dissipation in atomic quantum wires, Nat. Phys. **7**, 971 (2011).
[17] F. Ferri, R. Rosa-Medina, F. Finger, N. Dogra, M. Soriente, O. Zilberberg, T. Donner, and T. Esslinger, Emerging Dissipative Phases in a Superradiant Quantum Gas with Tunable Decay, Phys. Rev. X **11**, 041046 (2021).
[18] D. Nagy, G. Szirmai, and P. Domokos, Critical exponent of a quantum-noise-driven phase transition: The open-system Dicke model, Phys. Rev. A **84**, 043637 (2011).
[19] B. Öztop, M. Bordyuh, O. E. Müstecaplıoğlu, and H. E. Türeci, Excitations of optically driven atomic condensate in a cavity: Theory of photodetection measurements, New J. Phys. **14**, 085011 (2012).
[20] F. Brennecke, R. Mottl, K. Baumann, R. Landig, T. Donner, and T. Esslinger, Real-time observation of fluctuations at the driven-dissipative Dicke phase transition, Proc. Natl. Acad. Sci. U.S.A. **110**, 11763 (2013).
[21] L. Pezzè, A. Smerzi, M. K. Oberthaler, R. Schmied, and P. Treutlein, Quantum metrology with nonclassical states of atomic ensembles, Rev. Mod. Phys. **90**, 035005 (2018).
[22] J. Ma, X. Wang, C. Sun, and F. Nori, Quantum spin squeezing, Phys. Rep. **509**, 89 (2011).
[23] K. C. Cox, G. P. Greve, J. M. Weiner, and J. K. Thompson, Deterministic Squeezed States with Collective Measurements and Feedback, Phys. Rev. Lett. **116**, 093602 (2016).
[24] R. J. Lewis-Swan, M. A. Norcia, J. R. K. Cline, J. K. Thompson, and A. M. Rey, Robust Spin Squeezing via Photon-Mediated Interactions on an Optical Clock Transition, Phys. Rev. Lett. **121**, 070403 (2018).
[25] A. Shankar, J. T. Reilly, S. B. Jäger, and M. J. Holland, Subradiant-to-Subradiant Phase Transition in the Bad Cavity Laser, Phys. Rev. Lett. **127**, 073603 (2021).
[26] M. Boneberg, I. Lesanovsky, and F. Carollo, Quantum fluctuations and correlations in open quantum Dicke models, Phys. Rev. A **106**, 012212 (2022).
[27] F. Carollo, Non-Gaussian dynamics of quantum fluctuations and mean-field limit in open quantum central spin systems, arXiv:2305.15547.
[28] M. Tavis and F. W. Cummings, Exact solution for an *N*-molecule—radiation-field Hamiltonian, Phys. Rev. **170**, 379 (1968).
[29] R. H. Dicke, Coherence in spontaneous radiation processes, Phys. Rev. **93**, 99 (1954).
[30] J. Hu, W. Chen, Z. Vendeiro, A. Urvoy, B. Braverman, and V. Vuletić, Vacuum spin squeezing, Phys. Rev. A **96**, 050301(R) (2017).
[31] S. J. Masson, M. D. Barrett, and S. Parkins, Cavity QED Engineering of Spin Dynamics and Squeezing in a Spinor Gas, Phys. Rev. Lett. **119**, 213601 (2017).
[32] See Supplemental Material at http://link.aps.org/supplemental/10.1103/PhysRevLett.131.143604 for details on the semiclassical model, the second-order cumulant expansion, the Husimi spin Q function, and the quench protocol. Supplemental Material also includes Ref. [33].
[33] J. M. Radcliffe, Some properties of coherent spin states, J. Phys. A **4**, 313 (1971).
[34] M. Gross and S. Haroche, Superradiance: An essay on the theory of collective spontaneous emission, Phys. Rep. **93**, 301 (1982).
[35] A. V. Andreev, V. I. Emel'yanov, and Y. A. Il'inskiĭ, Collective spontaneous emission (Dicke superradiance), Sov. Phys. Usp. **23**, 493 (1980).
[36] A. Angerer, K. Streltsov, T. Astner, S. Putz, H. Sumiya, S. Onoda, J. Isoya, W. J. Munro, K. Nemoto, J. Schmiedmayer, and J. Majer, Superradiant emission from colour centres in diamond, Nat. Phys. **14**, 1168 (2018).
[37] M. Koppenhöfer, P. Groszkowski, H.-K. Lau, and A. A. Clerk, Dissipative superradiant spin amplifier for enhanced quantum sensing, PRX Quantum **3**, 030330 (2022).
[38] G. S. Agarwal, Master-equation approach to spontaneous emission, Phys. Rev. A **2**, 2038 (1970).
[39] N. Skribanowitz, I. P. Herman, J. C. MacGillivray, and M. S. Feld, Observation of Dicke Superradiance in Optically Pumped HF Gas, Phys. Rev. Lett. **30**, 309 (1973).
[40] J. Appel, P. J. Windpassinger, D. Oblak, U. B. Hoff, N. Kjærgaard, and E. S. Polzik, Mesoscopic atomic entanglement for precision measurements beyond the standard quantum limit, Proc. Natl. Acad. Sci. U.S.A. **106**, 10960 (2009).
[41] D. J. Wineland, J. J. Bollinger, W. M. Itano, F. L. Moore, and D. J. Heinzen, Spin squeezing and reduced quantum noise in spectroscopy, Phys. Rev. A **46**, R6797 (1992).
[42] D. J. Wineland, J. J. Bollinger, M. W. Itano, and D. J. Heinzen, Squeezed atomic states and projection noise in spectroscopy, Phys. Rev. A **50**, 67 (1994).

[43] M. A. Norcia, R. J. Lewis-Swan, J. R. K. Cline, B. Zhu, A. M. Rey, and J. K. Thompson, Cavity-mediated collective spin-exchange interactions in a strontium superradiant laser, Science **361**, 259 (2018).
[44] R. L. Devaney, Reversible diffeomorphisms and flows, Trans. Am. Math. Soc. **218**, 89 (1976).
[45] R. I. Bandara, A. Giraldo, N. G. R. Broderick, and B. Krauskopf, Infinitely many multipulse solitons of different symmetry types in the nonlinear Schrödinger equation with quartic dispersion, Phys. Rev. A **103**, 063514 (2021).
[46] M. Gärttner, J. G. Bohnet, A. Safavi-Naini, M. L. Wall, J. J. Bollinger, and A. M. Rey, Measuring out-of-time-order correlations and multiple quantum spectra in a trapped-ion quantum magnet, Nat. Phys. **13**, 781 (2017).
[47] D. Linnemann, H. Strobel, W. Muessel, J. Schulz, R. J. Lewis-Swan, K. V. Kheruntsyan, and M. K. Oberthaler, Quantum-Enhanced Sensing Based on Time Reversal of Nonlinear Dynamics, Phys. Rev. Lett. **117**, 013001 (2016).
[48] S. Colombo, E. Pedrozo-Peñafiel, A. F. Adiyatullin, Z. Li, E. Mendez, C. Shu, and V. Vuletić, Time-reversal-based quantum metrology with many-body entangled states, Nat. Phys. **18**, 925 (2022).
[49] V. I. Arnol'd, *Ordinary Differential Equations* (Springer-Verlag, Berlin, 1992).
[50] P. Glendinning, *Stability, Instability and Chaos* (Cambridge University Press, Cambridge, England, 1994).
[51] H. J. Carmichael, *Statistical Methods in Quantum Optics II: Non-Classical Fields* (Springer, New York, 2008).
[52] H. J. Carmichael, *An Open Systems Approach to Quantum Optics* (Springer-Verlag, Berlin, 1993).
[53] M. E. Peskin and D. V. Schroeder, *An Introduction to Quantum Field Theory* (Westview Press, Boulder, 1995).
[54] K. J. Percus, Correlation inequalities for Ising spin lattices, Commun. Math. Phys. **40**, 283 (1975).
[55] R. Kubo, Generalized cumulant expansion method, J. Phys. Soc. Jpn. **17**, 1100 (1962).
[56] M. Kira and S. W. Koch, Cluster-expansion representation in quantum optics, Phys. Rev. A **78**, 022102 (2008).
[57] M. Sánchez-Barquilla, R. E. F. Silva, and J. Feist, Cumulant expansion for the treatment of light–matter interactions in arbitrary material structures, J. Chem. Phys. **152**, 034108 (2020).
[58] P. Kirton and J. Keeling, Superradiant and lasing states in driven-dissipative Dicke models, New J. Phys. **20**, 015009 (2018).
[59] J. Q. Quach, K. E. McGhee, L. Ganzer, D. M. Rouse, B. W. Lovett, E. M. Gauger, J. Keeling, G. Cerullo, D. G. Lidzey, and T. Virgili, Superabsorption in an organic microcavity: Toward a quantum battery, Sci. Adv. **8**, eabk3160 (2022).
[60] D. Plankensteiner, C. Hotter, and H. Ritsch, Quantum-Cumulants.jl: A Julia framework for generalized mean-field equations in open quantum systems, Quantum **6**, 617 (2022).
[61] Y.-X. Huang, M. Li, K. Lin, Y.-L. Zhang, G.-C. Guo, and C.-L. Zou, Classical-to-quantum transition in multimode nonlinear systems with strong photon-photon coupling, Phys. Rev. A **105**, 043707 (2022).
[62] F. Robicheaux and D. A. Suresh, Beyond lowest order mean-field theory for light interacting with atom arrays, Phys. Rev. A **104**, 023702 (2021).
[63] O. Rubies-Bigorda, S. Ostermann, and S. F. Yelin, Characterizing superradiant dynamics in atomic arrays via a cumulant expansion approach, Phys. Rev. Res. **5**, 013091 (2023).
[64] C. Qu and A. M. Rey, Spin squeezing and many-body dipolar dynamics in optical lattice clocks, Phys. Rev. A **100**, 041602(R) (2019).
[65] F. Mivehvar, F. Piazza, T. Donner, and H. Ritsch, Cavity QED with quantum gases: New paradigms in many-body physics, Adv. Phys. **70**, 1 (2021).
[66] F. Finger, R. Rose-Medina, N. Reiter, P. Christodoulou, T. Donner, and T. Esslinger, Spin- and momentum-correlated atom pairs mediated by photon exchange, arXiv:2303.11326.
[67] M. H. Muñoz Arias, I. H. Deutsch, and P. M. Poggi, Phase-space geometry and optimal state preparation in quantum metrology with collective spins, PRX Quantum **4**, 020314 (2023).
[68] W. Kersten, N. de Zordo, O. Diekmann, T. Reiter, M. Zens, A. N. Kanagin, S. Rotter, J. Schmiedmayer, and A. Angerer, Triggered Superradiance and Spin Inversion Storage in a Hybrid Quantum System, Phys. Rev. Lett. **131**, 043601 (2023).